ISBN: 978-3-95450-202-8 doi:10.18429/JACoW-HB2018-MOP1WA01

J-PARC RCS: EFFECTS OF EMITTANCE EXCHANGE ON INJECTION PAINTING

H. Hotchi# and the J-PARC RCS beam commissioning group,
J-PARC Center, Japan Atomic Energy Agency, Tokai, Naka, Ibaraki, 319-1195 Japan

Abstract

The J-PARC 3 GeV rapid cycling synchrotron (RCS) is a high-power pulsed proton driver aiming for a 1 MW output beam power. This paper presents our recent efforts for beam dynamics issues that we faced during the RCS beam power ramp-up, especially about the optimization of the injection painting method in a situation involving the emittance exchange caused by the Montague resonance.

INTRODUCTION

The J-PARC 3 GeV rapid cycling synchrotron (RCS) is the world's highest class of a high-power pulsed proton driver aiming for a 1 MW beam power [1, 2]. A 400 MeV H^- beam from the injector linac is multi-turn charge-exchange injected into the RCS through a carbon foil over a period of 0.5 ms. The RCS accelerates the injected protons up to 3 GeV with a repetition rate of 25 Hz. Most of the RCS beam pulses are delivered to the materials and life science experimental facility (MLF), while only four pulses every several second are injected to the main ring synchrotron (MR) by switching the beam destination pulse by pulse.

The requirements for the beam operations to the MLF and the MR are different. Thus, different parameter optimizations are required for the two operation modes. Due to the higher operational duty, the machine activations of the RCS are mainly determined by the beam operation to the MLF. Therefore, a sufficient beam loss mitigation is required for this operation mode. In addition, for the MLF, a wide-emittance beam with low charge density is required to mitigate a shockwave on the neutron target, which is essential to obtain a sufficient lifetime of the neutron target. On the other hand, for the MR, a narrow-emittance beam with low beam halo is required contrary to the MLF case, which is essential to mitigate beam loss at the MR. In order to meet the different requirements for the beam operations to the MLF and the MR, we can utilize transverse injection painting [3], that is, applying large painting for the MLF and small painting for the MR.

Figure 1 shows the tune diagram around the operational point, in which the red lines represent the structure resonances up to 4th order derived from the three-hold symmetric lattice of the RCS, and the green circle shows the operational betatron tune that we had used until very recently. This operational point allows space-charge tune shifts to avoid serious structure resonances such as $\nu_{x,y} = 6$, $4\nu_{x,y} = 27$ and $2\nu_x + 2\nu_y = 27$, but, in exchange, it is very close to the Montague resonance $2\nu_x - 2\nu_y = 0$ [4]. As well known, the $2\nu_x - 2\nu_y = 0$ resonance, which is mainly excited by space-charge nonlinear fields such as octupole, causes emittance exchange. The emittance exchange has a major influence on the formation of the beam distribution during injection painting. This is the major issue in optimizing the injection painting for the MLF and the MR.

In this paper, the influence of the emittance exchange on injection painting and the optimization of the painting method in such a situation involving the emittance exchange are discussed for a high-intensity beam of 8.33 x 10^{13} ppp (1 MW-equivalent intensity). The present status of the RCS beam operation, optimized through the above discussion, and the future prospect are also mentioned in the latter part.

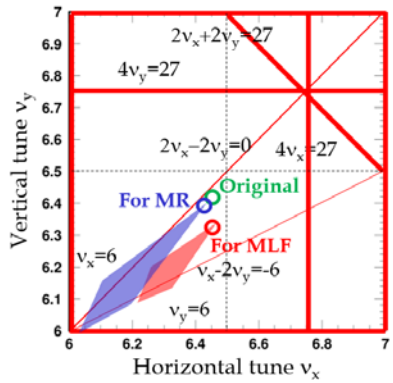

Figure 1: Tune diagram around the operational point.

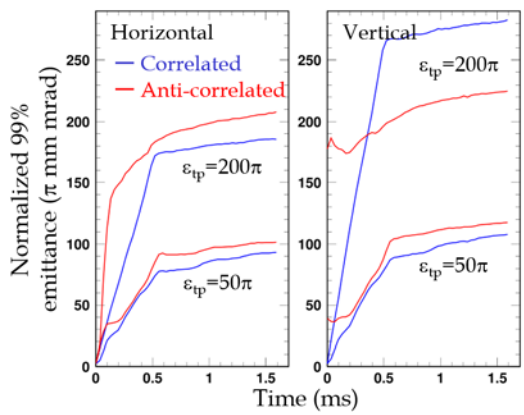

Figure 2: Time dependences of the beam emittances calculated for the first 1.5 ms.

EMITTANCE GROWTH DURING INJECTION PAINTING

In the RCS, both correlated painting and anti-correlated painting are available, and the painting emittance (ε_{tp}) is adjustable from 0 to 200π mm mrad for both the horizontal and the vertical planes [3], where ε_{tp} is defined as the un-

#hotchi.hideaki@jaea.go.jp

ISBN: 978-3-95450-202-8 doi:10.18429/JACoW-HB2018-MOP1WA01

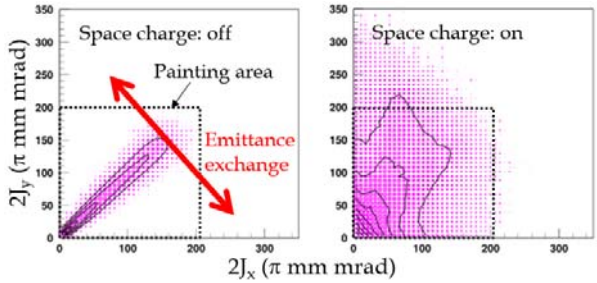

Figure 3: 2d plots of the betatron actions (J_x, J_y) at the end of injection calculated with the correlated painting of ε_{tp}=200π mm mrad.

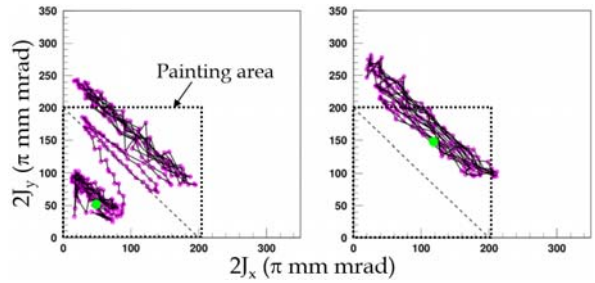

Figure 4: Single-particle motions during the correlated painting of ε_{tp}=200π mm mrad.

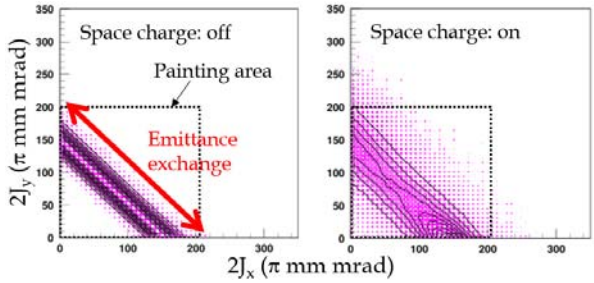

Figure 5: 2d plots of the betatron actions (J_x, J_y) at the end of injection calculated with the anti-correlated painting of ε_{tp}=200π mm mrad.

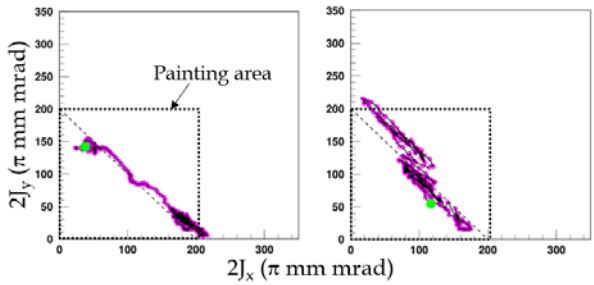

Figure 6: Single-particle motions during the anti-correlated painting of ε_{tp}=200π mm mrad.

normalized value of the entire painting area.

Figure 2 shows time dependences of the beam emittances for the first 1.5 ms calculated with ε_{tp} = 200π mm mrad and ε_{tp} = 50π mm mrad for correlated painting and anti-correlated painting. As shown in the figure, the correlated painting and the anti-correlated painting give the opposite result for the large painting and the small painting. In case of the large painting, the anti-correlated painting provides less emittance growth. But, in case of the small painting, the correlated painting rather than the anti-correlated painting gives narrower beam emittance. The opposite phenomena observed in the large painting and the small painting can be comprehended by considering the emittance exchange caused by the $2\nu_x - 2\nu_y = 0$ resonance, as is discussed below.

PARTICLE MOTIONS DURING LARGE PAINTING

First, we discussed the particle motions during injection painting with a large painting emittance of ε_{tp} = 200π mm mrad, which is required for the beam operation to the MLF.

Figure 3 shows a 2d plot of the betatron actions (J_x, J_y) at the end of injection calculated with the correlated painting of ε_{tp} = 200π mm mrad. As is shown in the left panel obtained with no space charge, in correlated painting, the injection beam is painted along the line of $J_x - J_y = 0$, namely, from the middle to the outside on both the horizontal and the vertical planes. This situation with no space charge significantly changes when the space charge is turned on, as shown in the right panel; one can see a significant diffusion of beam particles swerving from the path of beam painting. This large emittance dilution over the painting area is mainly caused by the emittance exchange. As illustrated in the left plot in Fig. 3, the directions of the beam painting and the emittance exchange are perpendicular to each other in case of correlated painting. This geometrical situation more directly leads the emittance exchange to significant emittance growths. Figure 4 shows a single-particle motion of one macro-particle leading to large emittance growths. It clearly shows that the emittance growth formed in the correlated painting is originated from the emittance exchange which occurs perpendicularly to the path of beam painting.

Figure 5 shows the case of the anti-correlated painting with ε_{tp} = 200π mm mrad. As is shown in the left panel obtained with no space charge, in anti-correlated painting, the injection beam is painted along the line of J_x+J_y=const., namely, from the middle to the outside on the horizontal plane, while, from the outside to the middle on the vertical plane. As illustrated in the left plot in Fig. 5, the direction of the anti-correlated painting is the same as that of the emittance exchange. Figure 6, displaying a single-particle motion of one macro-particle during the anti-correlated painting, clearly shows such a situation. This geometrical situation prevents the emittance exchange from causing large emittance growths. In the right panel in Fig. 5, one can confirm that most of the beam particles stay in the painting area even if the emittance exchange occurs, thanks to the same directions of the beam painting and the emittance exchange.

Thus, the emittance exchange has a different effect on the formation of the beam distribution depending on the

ISBN: 978-3-95450-202-8 doi:10.18429/JACoW-HB2018-MOP1WA01

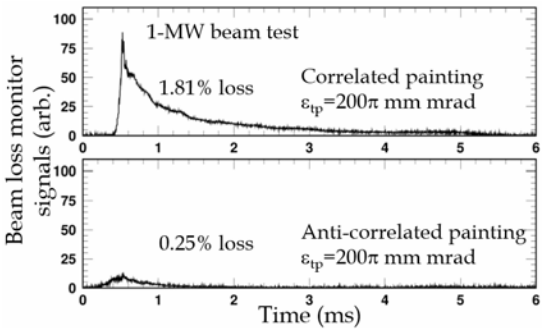

Figure 7: Beam loss monitor signals measured at the RCS collimator section.

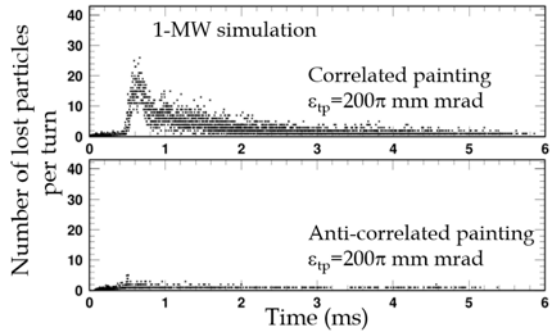

Figure 8: Numerical simulation results corresponding to the results of the 1 MW beam test in Fig. 7.

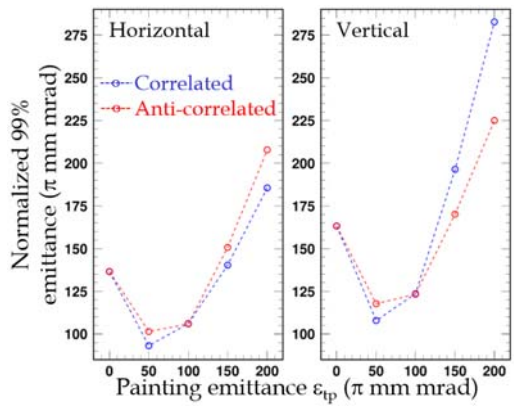

Figure 9: Beam emittances 1-ms after the end of injection calculated as a function of ε_{tp}.

geometrical relation between the beam painting and the emittance exchange in the (J_x, J_y) space. The above analysis concludes that the anti-correlated painting more favours the suppression of emittance growths caused by the emittance exchange. Figure 7 is the result of the 1 MW beam test [5], showing the beam loss monitor signals at the RCS collimator section. As shown in the figure, a significant beam loss was observed for the correlated painting with $\varepsilon_{tp} = 200\pi$ mm mrad. But, by introducing the anti-correlated painting with the same painting emittance, the beam loss was successfully reduced to the order of a couple of 10^{-3} as expected. This empirical situation was well reproduced by the numerical simulations, as shown in Fig. 8. Through the measurements and the numerical simulations, we confirmed the advantage of anti-correlated painting. But, we have to note that the conclusion here is just for the case of large painting.

PARTICLE MOTIONS DURING SMALL PAINTING

Next, we investigated the case of small painting, which is required for the beam operation to the MR.

Figure 9 shows the beam emittance 1-ms after the end of injection, calculated as a function of the painting emittance for correlated painting and anti-correlated painting. This dependence is ascribed to the balance between the painting emittance and its resultant space charge mitigation; they are well balanced at $\varepsilon_{tp} = 50\pi$ mm mrad, providing the minimum beam emittance there. In addition, in this figure, one can find the correlated painting rather than the anti-correlated painting achieves the narrower beam emittance at $\varepsilon_{tp} = 50\pi$ mm mrad. This situation for correlated painting and anti-correlated painting is completely opposite to the case of large painting. This characteristic phenomenon observed in the small painting is also understandable by considering the effect of the emittance exchange, as is discussed below.

In anti-correlated painting, the direction of the beam painting is the same as the direction of the emittance exchange. This geometrical situation well suppresses emittance growths directly caused by the emittance exchange, but it has a potential of causing a significant modulation of the charge density. Figure 10 shows a 2d plot of the betatron actions (J_x, J_y) during the anti-correlated painting with $\varepsilon_{tp} = 50\pi$ mm mrad. In this figure, one can find the formation of a high-density isle at the late stage of injection. This concentration of beam particles is ascribed to the synchronism between the beam painting and the move of the beam distribution caused by the emittance exchange, as shown in Fig. 11. But, such a significant charge density modulation is not found in the large painting, as shown in Fig. 5. The synchronism between the two motions is lost in going to larger painting, so a uniform distribution is relatively maintained in the large painting. That is, it can be said that the charge density modulation is a characteristic phenomenon enhanced in the anti-correlated painting with a small painting emittance.

Figure 12 shows the case of the correlated painting with $\varepsilon_{tp} = 50\pi$ mm mrad. In correlated painting, the emittance exchange occurs in the orthogonal direction to the path of beam painting. This geometrical situation enhances emittance growths simply caused by the emittance exchange itself, but, in exchange, it has the advantage of avoiding a modulation of the charge density, as shown in the figure.

These characteristic behaviours of beam particles during the small painting were experimentally confirmed as shown in Fig. 13; a high-density peak structure was found for the anti-correlated painting with $\varepsilon_{tp} = 50\pi$ mm mrad, while a more uniform beam distribution was observed for

ISBN: 978-3-95450-202-8 doi:10.18429/JACoW-HB2018-MOP1WA01

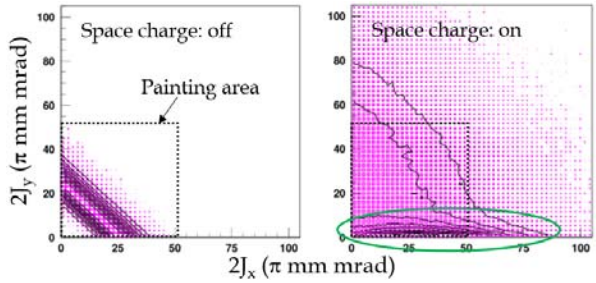

Figure 10: 2d plots of the betatron actions (J_x, J_y) at the end of injection calculated with the anti-correlated painting of ε_{tp}=50π mm mrad.

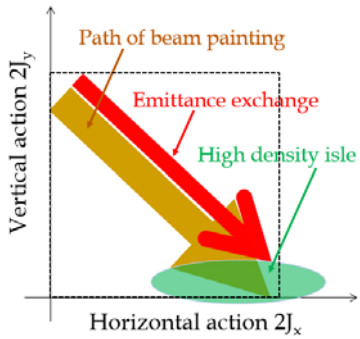

Figure 11: Schematic diagram of the geometrical relationship in the (J_x, J_y) space between the emittance exchange and the anti-correlated painting with a small painting emittance.

the correlated painting with ε_{tp} = 50π mm mrad, as predicted.

The high-density isle formed in the anti-correlated painting with ε_{tp} = 50π mm mrad causes a large space-charge detuning as shown in Fig. 14, leading to significant additional emittance growths afterward. The emittance growth caused via the formation of the high-density isle is more critical than that caused by the emittance exchange itself in the correlated painting. This is the main reason why the anti-correlated painting leads to larger emittance growths in case of ε_{tp} = 50π mm mrad.

RESULT OF DISCUSSION

The emittance exchange makes two major effects during injection painting. One (i) is the emittance growth simply caused by the direct effect of the emittance exchange, which is more enhanced in correlated paining. Another (ii) is from the secondary effect of the emittance exchange, namely, the emittance growth caused through a modulation of the charge density, which is more enhanced in anti-correlated painting. In large painting such as ε_{tp}=200π mm mrad, the former effect (i) is more significant, so anti-correlated painting, suppressing the effect (i), leads to less beam loss. On the other hand, in small painting such as ε_{tp} = 50π mm mrad, the latter effect (ii) is more critical, so correlated painting avoiding the effect (ii), leads to less emittance growth.

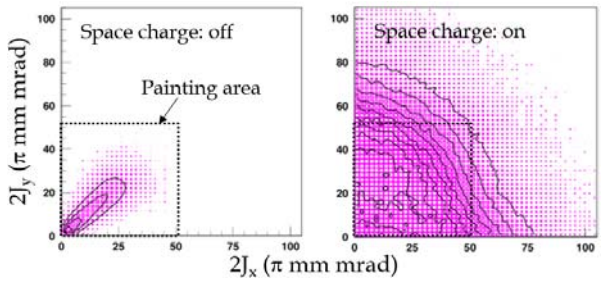

Figure 12: 2d plots of the betatron actions (J_x, J_y) at the end of injection calculated with the correlated painting of ε_{tp}=50π mm mrad.

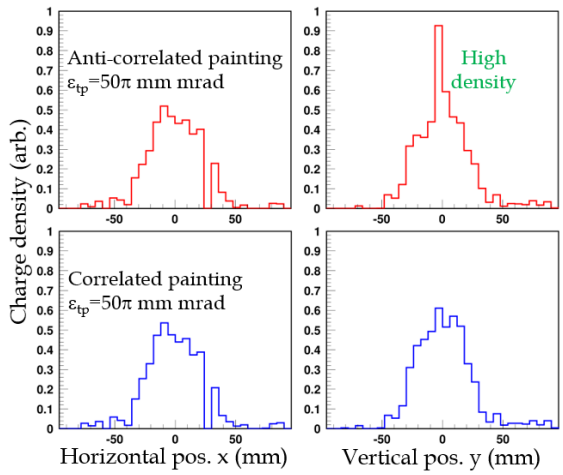

Figure 13: Beam profiles measured at the end of injection.

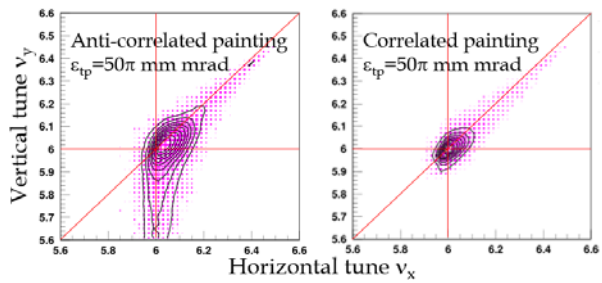

Figure 14: Space-charge tune shifts calculated at the end of injection.

PRESENT STATUS AND FUTURE PROSPECT OF RCS BEAM OPERATION

Based on the above result, we optimized the operational parameters including injection painting for the MLF and the MR, which are now applied for the routine user operations.

For the MLF, the betatron tune is now set to (6.45, 6.32) as shown in Fig. 1 (red circle), where the large painting with ε_{tp} = 200π mm mrad is applied. This operational point is relatively far from the $2\nu_x - 2\nu_y = 0$ resonance, so the effect of the emittance exchange is not critical. Therefore, the correlated painting as well as the anti-correlated

ISBN: 978-3-95450-202-8 doi:10.18429/JACoW-HB2018-MOP1WA01

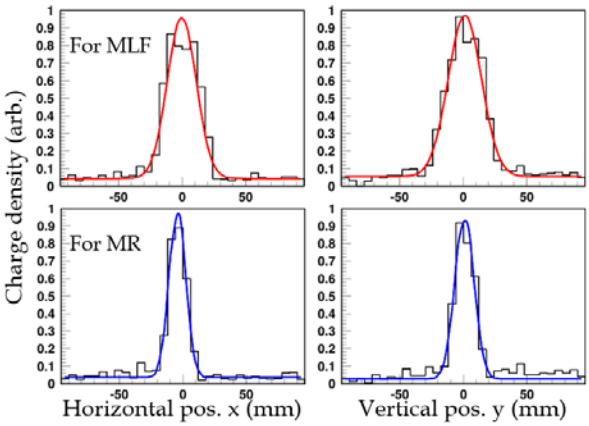

Figure 15: Beam profiles measured at extraction.

painting are now feasible for the MLF.

For the MR, the operational point is set to (6.42, 6.40) as shown in Fig. 1 (blue circle), where the small painting with $\varepsilon_{tp} = 50\pi$ mm mrad is applied. This small painting causes a large space-charge detuning, so a part of beam particles possibly reaches the integers of $\nu_{x,y} = 6$ as illustrated by a blue necktie in Fig. 1. The integers involve all-order systematic resonances and strongly affect the beam. This operational point provides a larger separation from $\nu_{x,y} = 6$, but it is very close to $2\nu_x - 2\nu_y = 0$; the beam suffers heavy effects of the emittance exchange in exchange for less effects of $\nu_{x,y} = 6$. Therefore, we are now applying the correlated painting for the MR. As discussed in the last section, the correlated painting more favours the suppression of emittance growths originating from the emittance exchange in case of small painting such as $\varepsilon_{tp} = 50\pi$ mm mrad.

To realize the optimal beam operations for the MLF and the MR compatibly, we have recently introduced a pulse-by-pulse switching of the operational parameters according as the beam destination [6]; the pulse-by-pulse switching of the betatron tune is conducted with 6 sets of pulsed trim quadrupole magnets, while the pulse-by-pulse switching of the injection painting is performed with 6 sets of pulsed injection bump magnets. By optimizing the operational parameters for each beam destination, and, in addition, by realizing their pulse-by-pulse switching, we successfully met the requirements for the MLF and the MR; a wide-emittance beam for the MLF and a narrow-emittance beam for the MR were achieved as requested while keeping beam loss within acceptable levels, as shown in Fig. 15.

Thus, the accelerator itself is now ready to try a continuous 1 MW beam operation for the MLF. But, unfortunately, we had troubles in the liquid mercury targets used for neutron production at the MLF; a water leak from the target vessel happened two times one after another at the 500 kW beam power in 2015 - 2016. Therefore, since then, the routine beam power had been limited to 150~200 kW. But, in the last summer maintenance period in 2017, a new robust target was installed, so we are now back to the beam power ramp-up phase again. While the present beam power for the MLF users is 500 kW, it will be increased step by step to 1 MW from now on carefully monitoring the condition of the target.

The RCS is now delivering the beam to the MR at a beam intensity of ~ 6.5 x 10^{13} ppp corresponding to 78% of the RCS design intensity. With this beam, the MR has recently achieved a new record of a 500 kW beam power for the neutrino experiment via the recent efforts for beam loss reduction including the improvement of the RCS beam quality [6, 7]. The design beam power of the MR is 750 kW. To achieve the design value and more, the MR operation cycle time will be reduced from 2.48 s to 1.3 s in the near future. Hardware upgrades to get such a rapid operation cycle, such as the upgrade of the main magnet power supplies, is in progress now.

SUMMARY

The effects of the emittance exchange on injection painting were investigated for a 1 MW-equivalent beam intensity. In this work, we found the emittance exchange makes two major effects during injection painting;

(i) Emittance growth directly caused by the emittance exchange itself.

(ii) Emittance growth caused by the secondary effect of the emittance exchange, namely, via a modulation of the charge density.

They each are enhanced or mitigated depending on the choice of correlated painting and anti-correlated painting, and their painting emittance. In a situation with the emittance exchange, investigating the particle motions while considering the geometrical relation in the (J_x, J_y) space between the beam painting and the emittance exchange is a key to optimizing the injection painting as well as to understanding the behavior of the beam. Based on the analysis result, the operational parameters including injection painting for the MLF and the MR were recently re-optimized, which are now successfully applied for the routine user operations.

REFERENCES

[1] High-intensity Proton Accelerator Project Team, "Accelerator Technical design report for high-intensity proton accelerator facility project, J-PARC", Rep. JAERI-Tech-2003-044, JAERI, Tokai, Japan, Mar. 2003.

[2] H. Hotchi *et al.*, "Beam commissioning of the 3 GeV rapid cycling synchrotron of the Japan Proton Accelerator Research Complex", *Phys. Rev. ST Accel. Beams*, vol. 12, p. 040402, Apr. 2009, doi:10.1103/PhysRevSTAB.12.040402

[3] H. Hotchi *et al.*, "Beam loss reduction by injection painting in the 3 GeV rapid cycling synchrotron of the Japan Proton Accelerator Research Complex", *Phys. Rev. ST Accel. Beams*, vol. 15, p. 040402, Apr. 2012, doi:10.1103/PhysRevSTAB.15.040402

[4] B.W. Montague, "Fourth-order coupling resonance excited by space-charge forces in a synchrotron", CERN, Geneva, Switzerland, Rep. CERN-68-38, Oct. 1968.

ISBN: 978-3-95450-202-8 doi:10.18429/JACoW-HB2018-MOP1WA01

[5] H. Hotchi *et al*., "Achievement of a low-loss 1 MW beam operation in the 3 GeV rapid cycling synchrotron of the Japan Proton Accelerator Research Complex", *Phys. Rev. Accel. Beams*, vol. 20, p. 060402, Jun. 2017, doi:10.1103/PhysRevAccelBeams.20.060402

[6] H. Hotchi *et al*., "Pulse-by-pulse switching of operational parameters in J-PARC 3 GeV RCS", in *Proc. IPAC'18*, Vancouver, Canada, Apr. 2018, paper TUPAL018.

[7] S. Igarashi *et al*., "High-power beam operation at J-PARC", presented at HB2018, Daejeon, Korea, Jun. 2018, paper TUA2WD02, this conference.